Application of Landscape Analysis Techniques on the Oral Structures of the American Shad

Cassandra L. Chang

Abstract

Landscape analysis techniques may be used to distinguish patterns in the gill rakers of the American shad. To better understand the functional morphology of the gill rakers, a lacunarity analysis was performed on the epibranchial and ceratobranchial sections of the four main gill arches in the oral cavity of the shad. Lacunarity has previously been used to characterize landscapes, and using varying sizes and shapes of extents may reveal new patterns and quantify the structure of the gill rakers. The circular and square windows detected the same patterns in the gill rakers, which validated the curves. The lacunarity curves for the epibranchial and ceratobranchial sections showed different patterns when normalized and compared. Lacunarity values also differed in range between arches, but maintained the same general curve characteristics. The fluid exit area was also quantified using landscape area techniques to understand general flow movement and filter mechanics in the shad. This area was compared to previous exit ratios calculated using the gape and opercular areas. The rakers were shown to block about 50% of the total area between the oral and opercular areas, which matches the previous approximate fluid exit ratio of 2:1. Further analyses may be conducted on a larger sample size to verify our findings, and the results may be used to design an efficient crossflow filter for use in industry.

Introduction

The American shad (*Alosa sapidissima*) is an anadromous fish species in the family *Clupeidae*. The shad is a ram suspension feeder and feeds on its prey, such as zooplankton, copepods, and larval fish, by swimming with an open mouth and allowing water to flow into the gape and through the oral cavity to the opercular cavity. The filter surface in the shad, consisting of structures called gill rakers which protrude from the gill arches opposite the gill filaments, partially obstructs the flow and separates the food particles from the water. Each gill raker has several small bumps or points on them, called denticles, that increase the surface area and boundary layer of the rakers (Figure 1).

It has previously been assumed that the gill rakers function as a dead-end sieve (Gibson 1988), where water encounters the filter surface perpendicularly and the particles are trapped on the filter surface. The limitations of a dead-end sieve filtration system are that the particles captured on the surface must be larger than the spaces in the filter surface, and that capturing particles directly leads to clogging the filter. To utilize this type of filter mechanism, the shad must also have a method to clear the filter and move the particles to the back of the oral cavity where they can be swallowed. However, Sanderson et al. (2001) found in their study that the shad use crossflow filtration in their oral cavities to separate particles from the water. In crossflow filtration, the bulk water flow is parallel to the filter surface, and water escapes perpendicularly through the filter surface as the flow continues across the surface, leading to a concentrated slurry of particles at the end. This method of filtration is extremely efficient and is less likely to clog than a dead-end sieve filter. It can also trap particles that are much smaller than the gaps in the filter surface, which filter-feeding fish are able to do. For the shad, the gill

rakers (the filter surface) direct this slurry to the oesophagus at the back of the oral cavity where it can then swallow and consume its prey.

Filters that do not clog are vital in industries such as pharmaceuticals and biotechnology. A clogged filter takes time and resources to clean and reuse, which comes at a high price. Fish are extremely efficient at filtering their prey without clogging, as that may lead to serious complications or death, so they may be a good model for a high efficiency industrial filter. In order to replicate this type of filter, we must fully understand the structure of the gill rakers and its effect on its function as a filter.

In this study, we conducted a spatial analysis of the gill rakers to better understand its function as a filter surface. Small patterns in the gill rakers may affect the fluid flow in this region. A lacunarity curve for each of the various sections of the gill arches was produced and analyzed to determine if there is a particular spatial pattern that allows the gill rakers to work as a filter at maximum efficiency. Lacunarity has been used in previous studies to quantify the patterns in a landscape (Leu and Hanser 2008). A convex curve shows a clumped distribution, while a concave curve shows a dispersed distribution (Leu and Hanser 2008). Using this index on the gill rakers may reveal a pattern that has not been previously quantified or observed. In addition, the area in between the rakers was quantified to estimate the fluid exit area and to assist in the understanding of water flow movement in the oral and opercular cavities of the shad. Previous studies have attempted to quantify the gap size and raker size indirectly (Hammann 1985) but have not fully quantified the area between the rakers.

Methods

Lacunarity Analysis

An American shad head was obtained, preserved in formalin, and stored in ethanol. Each of the four gill arches on the left side of the fish (Figure 2) were removed using scissors and forceps, cutting as close to the midlines on the top and bottom of the mouth as possible to maintain the integrity of the arch structure (Figure 3). Images were taken of each arch in full, with gill filaments attached. Each arch was then separated at the epibranchial-ceratobranchial joint, where the ridges on the gill arch change angle (Figure 3). The epibranchial and ceratobranchial sections were photographed such that most of the edges of the gill rakers lay flat along the surface and the denticles on at least one side of the gill rakers were visible (Figure 3).

The images were loaded into ArcMap and converted to black and white by importing only one band from each image, typically the red band (Figure 4a). The main gill raker extent was separated from the rest of the arch and background. This extent was converted into a binary raster with the gill rakers, classified as 1, separated from the inter-raker space, classified as 0 (Figure 4b). The threshold was determined visually (Appendix A). A moving window analysis was then performed to obtain lacunarity values. A moving window analysis takes the statistics within a particular extent – in this case, the sum of all the values within the extent. Circular windows with radii of 1, 10, 50, 100, 200, 400, 800, 1000, and 2000 cells were used as the extent in the analysis. Since the rakers show a repeating linear pattern, a square window with sides of length 2, 18, 89, 177, 354, 709, 1418, 1772, and 3545 were also used, such that the areas within the windows were approximately equal to the corresponding circular window areas, to potentially further detect patterning. The mean and variance for each moving window analysis were exported into a spreadsheet for calculation.

Lacunarity, a landscape index to measure dispersal and quantify patterning, was calculated for each moving window analysis and used to determine patterning within the gill rakers. Lacunarity was calculated using the equation

$$lacunarity = \frac{\sigma}{\bar{x}^2} + 1 \quad (1)$$

where σ represents the variance and $\bar{x}$ represents the mean (Leu and Hanser 2008). When plotted on a natural log graph, the convexity or concavity of the lacunarity curve reveals the type of landscape shown. The curves can reveal how dispersed or clumped the landscape is and help quantitatively describe the patterns found. This index may find patterns that the human eye could not detect on its own.

Fluid Exit Ratio Quantification

Each of the epibranchial and ceratobranchial sections of the first three gill arches were divided into two or three segments for ease of photography and the ability to rotate each section such that the edge of the rakers lay as flat as possible along the surface (Figure 5). This allowed images taken to show the true space between the rakers as best as possible, leaving as little of the rakers rotated to block space. Images were taken directly above each section with a millimeter scale bar included for conversion.

These images were loaded into ArcMap and converted to black and white by taking one color band, typically the red band (Figure 4a). The image was then cut to include only the rakers from the base to the tip and the area between them. This new portion was converted into a binary raster, with 1 representing an area with gill rakers and 0 representing an area in the inter-raker space (Figure 4b). The threshold was determined visually (Appendix A). Counts for each area were obtained in terms of cells and added between the sections to obtain total raker area, total open area, and total overall area. The counts were then converted into square millimeters using

the scale bar in the image. Ratios between the open area and the total area, and the raker area and the total area were calculated.

Results

The lacunarity values and the moving window size were plotted on a natural-log graph. The radius of the window was used in the circular windows and the side length was used in the square windows. The lacunarity curves for each section of each arch using the square and circular windows are presented together in Figure 6a-h. The geometry of the window did not appear to affect the overall shape of the lacunarity curve. Since the natural pattern of the gill rakers is linear and more box-like, a square window may catch more patterning in its area. However, as shown in Figure 6a-h, the lacunarity curves retain the same characteristics and the circular and square windows captured the same pattern in the gill rakers. The slight discrepancies in the graphs may be attributed to the rounding that occurred when calculating the side length for the square windows. The moving window analysis required a whole number of cells for each side. Slight changes in the size and shape of area will affect total lacunarity, but the small magnitude of the change and the consistency in the curves from the first arch to the fourth arch show that the shape of the moving window does not affect the spatial analysis in our study and that the windows were able to capture the same distinct patterns. The remaining lacunarity analyses were performed on the circular window results.

The lacunarity curves for the ceratobranchial and epibranchial portions of the gill arches are presented in Figures 8 and 9. These curves each show two maxima. In most landscape analyses, the lacunarity curves tend to only decrease, with the point of slope change representing the scale of nestedness, where patterns repeat themselves and the variance decreases. However,

in the gill rakers, the curves decrease at a constant slope, then increase again before finally decreasing and approching zero.

The epibranchial and ceratobranchial curves differ from each other as well. The plots comparing the normalized ceratobranchial and epibranchial lacunarity curves for each arch are presented in Figure 7a-d. The lacunarity curves for the epibranchial sections tended to increase and decrease more drastically than the ceratobranchial sections. Both curves change slope initially at the same point, with the epibranchial curve increasing and the ceratobranchial curve decreasing. Both curves approach zero at the end.

The fluid exit area in square millimeters and ratio for each arch is presented in Table 1. The percent of open area tends to decrease as the arch gets smaller, with the fourth arch at the back of the mouth having the smallest percent of open area. Overall, the rakers appear to cover half of the area between the oral and opercular cavities.

Discussion

The increase in slope in the lacunarity curves in the ceratobranchial and the epibranchial portions of each arch show the scale of a single gill raker. The increase in variance corresponds to a radius of 50. In Figure 10, we see that extents with radii or sides of 10 cells and smaller would remain within one raker, but radii of 50 cells and higher reach both raker and inter-raker space. This would increase the variance in the windows with a radius or side length longer than 50 cells, until the extent grew enough to include more of the rakers and thus allow the variance to stabilize. The rakers also tend to taper from the base (where they attach to the gill arch) to the tips. The space between the rakers is not equal from base to tip, and therefore varies from one side of the image to the next. This tapering and consistent variance of the raker and open space

pattern may also affect the lacunarity values. The repeated parallel orientation of the rakers and the denticles form a distinct pattern that is captured in this curve.

The variations between the lacunarity curves for the epibranchial and ceratobranchial portions of the gill arch (Figure 7a-d) may be attributed to the variation in size and overall shape. The epibranchial section tends to be much smaller and have a more triangular shape, while the ceratobranchial section tends to be longer and more rectangular in shape. The epibranchial section and the ceratobranchial sections are also oriented differently in the oral cavity, which may lead to a different tilt or orientation of the gill rakers. The rakers may also differ slightly in width or taper differently in the two sections, distinctions that are difficult to observe visually. The smaller size and higher variation in the spread of the rakers and inter-raker space may cause a much higher increase in variance across different extent, while the slightly higher consistency of the raker patterns in the ceratobranchial portions may lead to more muted changes in variance and the lacunarity curve across different extents.

Lacunarity curves also varied within each section between different arches (Figures 8, 9). Although all of the curves exhibited the same general behaviors, the magnitude of the lacunarity values and the intercept changed as the arches changed. For the ceratobranchial sections, the intercept decreased as the arches progressed from the front to the back of the oral cavity. Variance likely decreases in this way as the arches progressively get smaller from the front to the back of the oral cavity, and the rakers tilt so that they are closer together. Some errors in imaging, which increased as the arches decreased in size, may also create large sections or patches of what appears to be entirely rakers, when in reality there are small spaces between these rakers. This would decrease the variance in the patterns as well. In the epibranchial sections, the curves vary more in shape, but hold the same major characteristics. Similarly, the

intercept tends to decrease as the arch decreases in size, except for the fourth (and smallest) arch, which had a relatively high intercept. Again, errors in imaging may cause this increase in variance, as well as the overall tilt of the rakers.

The fluid exit ratio tended to decrease as the arches decreased in size. This matches the hypothesis of crossflow filtration, as more water would encounter the first arch, as it is closest to the gape, than the fourth arch, as most fluid would have already exited the oral cavity at that point. The residual amount of water would need less area to escape than the main bulk flow. In an ongoing study by Chang et al., gape area was found to be approximately 1240 square millimeters, with the fluid exit ratio (the ratio of open gape area to open opercular area) to be approximately 1:2. This corresponds with the results of the fluid exit ratio found in this study, as the gill rakers separate the oral and opercular cavities. The total quantified area in this study is much larger than the gape area found previously, which may raise concern. However, the gill arches and rakers are not oriented perpendicularly to the gape, instead oriented at an angle on either side forming a curved branchial basket shape. In this study, the rakers were laid flat instead of at an angle, as the water may travel outwards once in the oral cavity of the fish. However, it would likely encounter the rakers at an angle, which would reduce the total area of the rakers. The projection of the rakers accounts for this large discrepancy in the entrance area calculations.

Future studies based on this research would include testing the lacunarity patterns of artificial raker models, to see if the particular angle, twist from base to tip, or tapering rate from base to tip affect the shape of the curve. Recreating the curves measured in this study using artificial models would also assist in the formation of filters that can operate as efficiently as the gill rakers in the shad. It is important to link the lacunarity to the structure itself and its filtering

capacity. Another topic of interest would be comparing the lacunarity curves of gill rakers between different species of fish, as well as different types of feeders. Lacunarity curves for all ram suspension feeding fish may look similar, while curves for suction or deposit feeding fish may look different. Although there are many different morphologies of gill rakers, the lacunarity index and analysis may prove to be useful in finding patterns that are not distinguishable by observation and measurement alone.

Literature Cited

Chang, C. L., Sanderson, S. L., Hwang, J. D., and Findley, B. [Flow Interactions in the Oral and Opercular Cavities in the American Shad]. Unpublished raw data.

Hammann. M. G. (1985) The developmental morphology of the filtering apparatus in American shad (*Alosa sapidissima*), a planktivorous fish: a preliminary study. *Ciencias Marinas 11*(3): 5-20.

Gibson, R. N. (1987) Development, morphometry and particle retention capability of the fill rakres in the herring, *Clupea harengus* L. *Journal of Fish Biology 1988*(32), 949-962.

Mummert, J. R. and Drenner, R. W. (1986) Effect of Fish Size on the Filtering Efficiency and Selective Particle Ingestion of a Filter-Feeding Clupeid. *Transactions of the American Fisheries Society 115*: 522-528. DOI: 10.1577/1548-8659(1986)115<522:EOFSOT>2.0CO;2

Leu, M. and Hanser, S. E. (2011). Influences of the human footprint on sagebrush landscape patterns: implications for sage-grouse conservation. In S. T. Knick and J. W. Connelly (Eds.), *Studies in Avian Biology* vol. 38 (pp. 253-271) Berkeley, CA: University of California Press.

Sanderson, S.L., Cheer, A. Y., Goodrich, J. S., Graziano, J. D. and Callen, T. W. (2001) Crossflow filtration in suspension-feeding fishes. *Nature 412*(6845):439-41. DOI: 10.1038/35086574

Figures

Figure 1. Detail of the gill rakers. The epibranchial portion of the first arch is shown in the image. The gill ridges, filaments, rakers, denticles, and the arch are labeled. Note the shape and the orientation of the rakers.

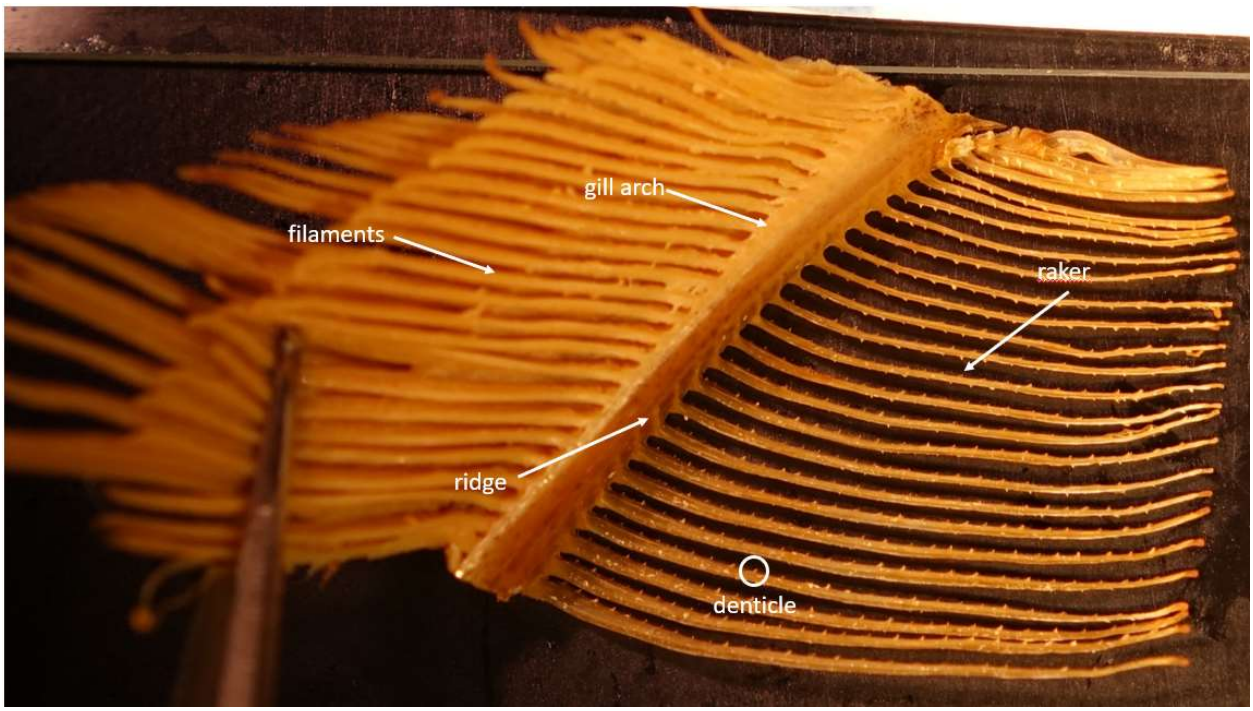

Figure 2. Image of the oral cavity through the gape of the American shad. The different gill arches are labeled. Note the orientation of the gill rakers and arches.

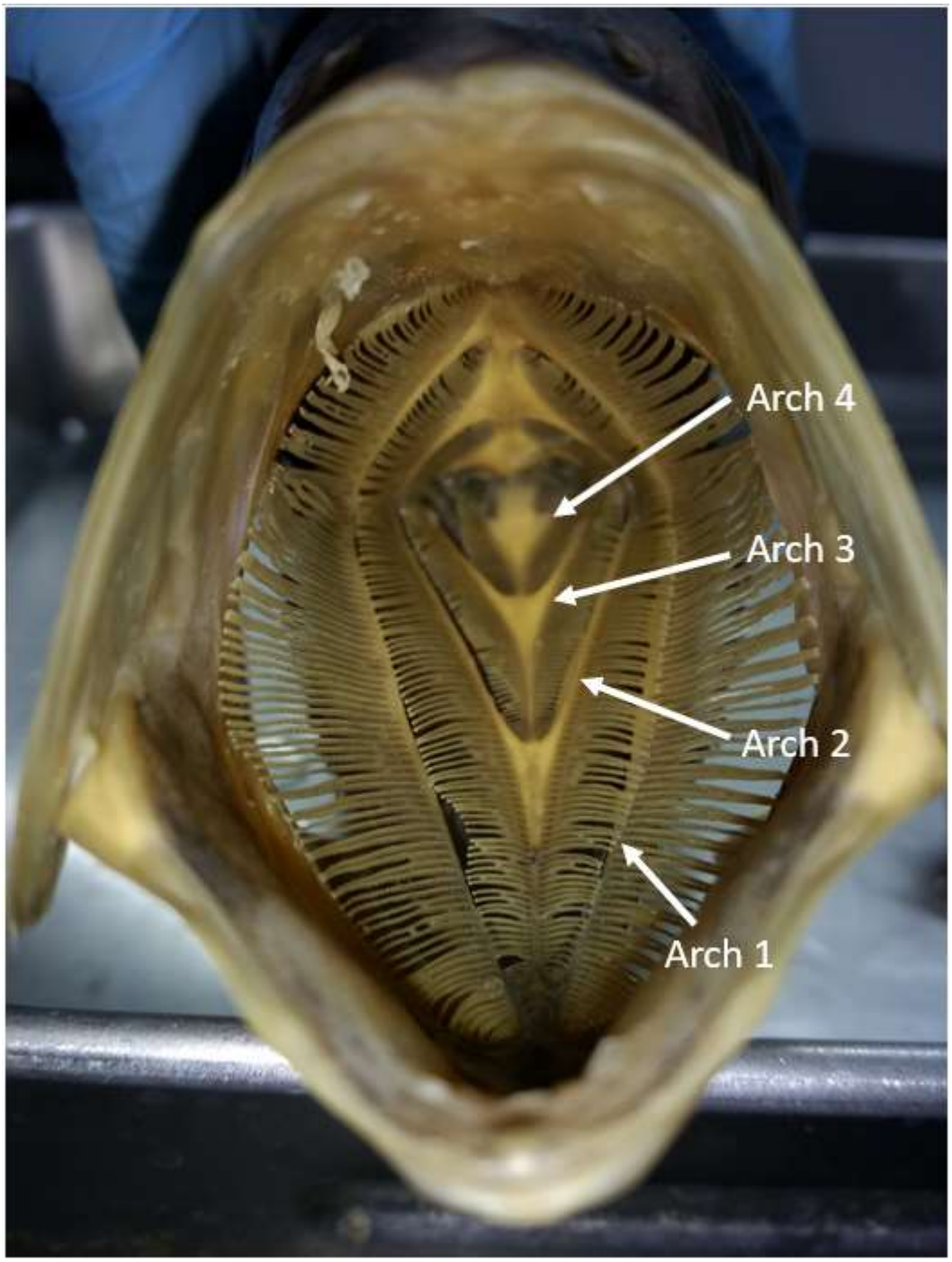

Figure 3. Detail of a gill arch. Each gill arch has the same overall structure, but differs in size. The arch pictured is the first gill arch (the largest one). The epibranchial portion is connected to the roof of the mouth while the ceratobranchial portion is connected to the floor of the mouth. The epibranchial-ceratobranchial joint is defined as the point where the two sections meet, and can be distinguished by a change in the ridge angle on the arch.

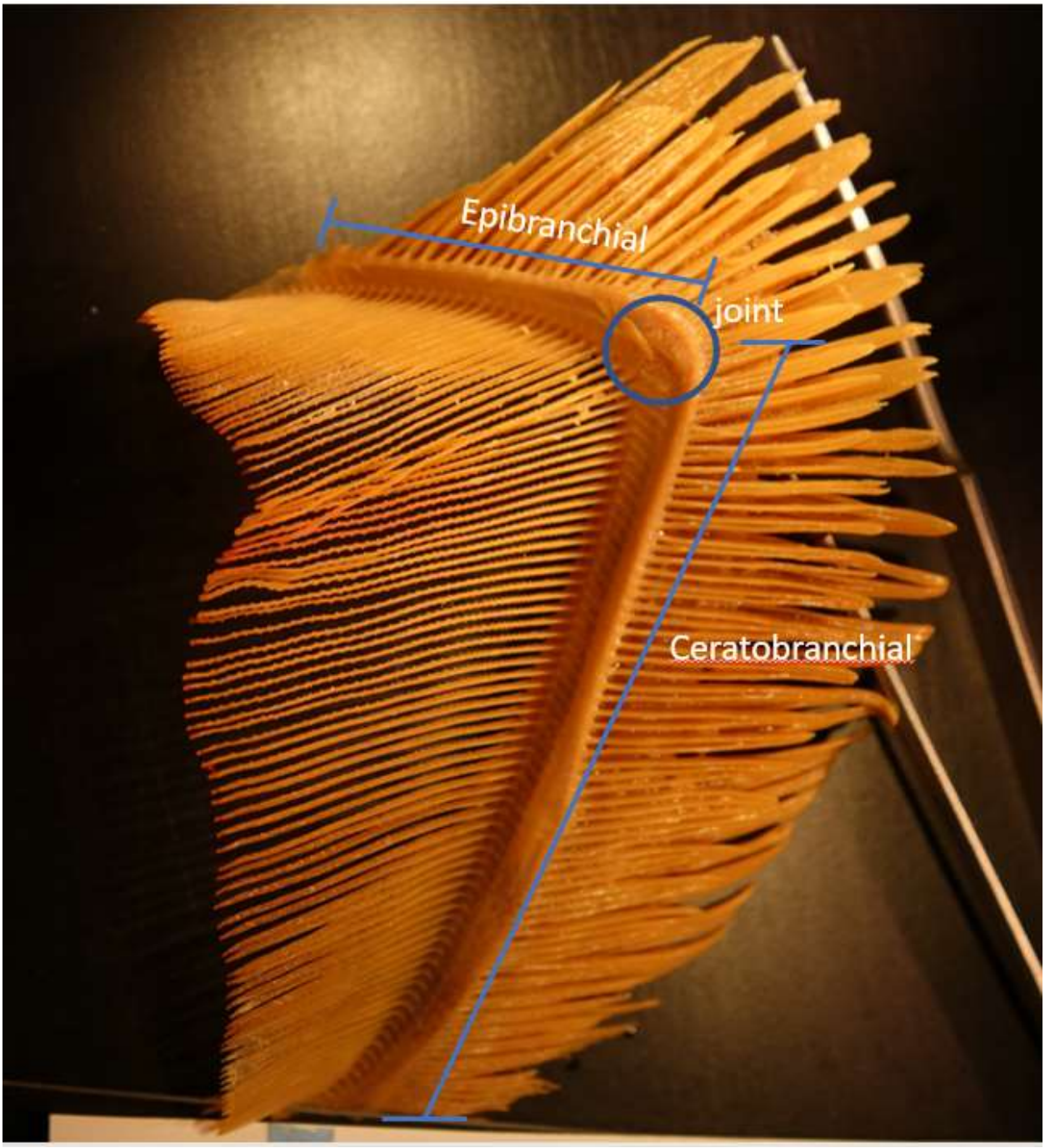

Figure 4. The image processing method. Figure 4a shows the black and white image, and Figure 4b shows the binary raster of the rakers taken from 4a. The epibranchial section of the first arch is shown as the example.

a.

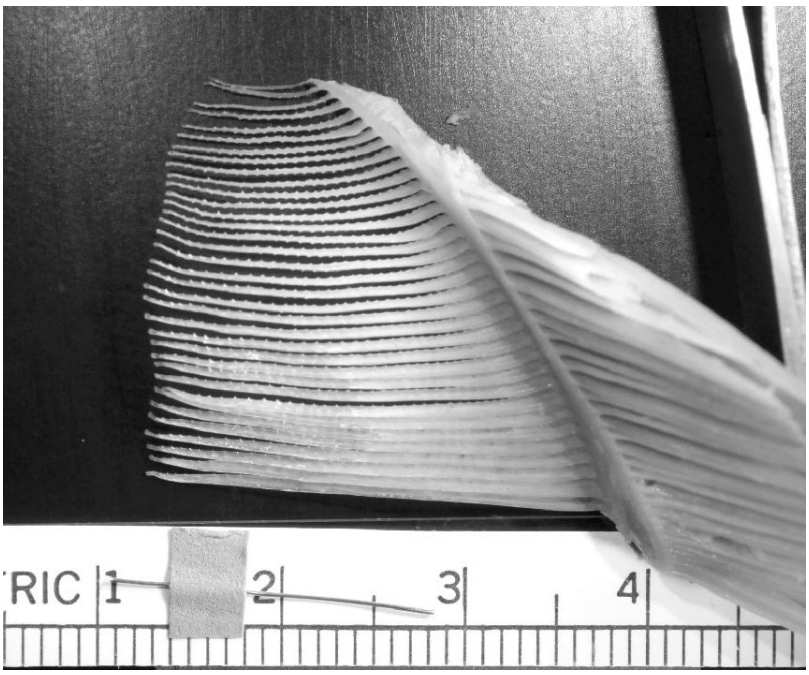

b.

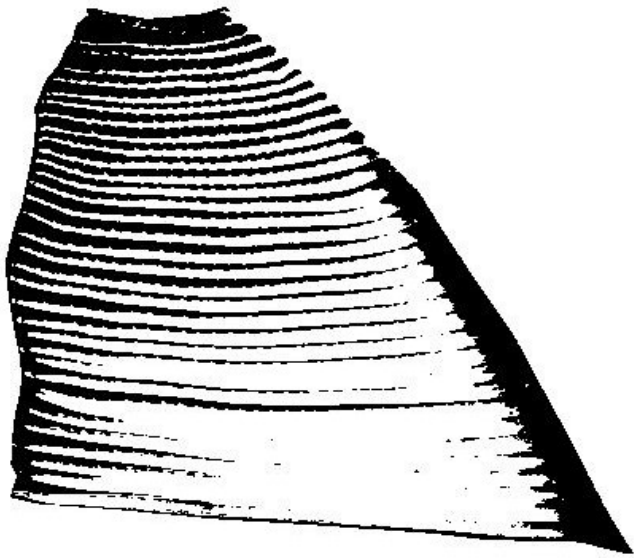

Figure 5. The first ceratobranchial section split into three portions for accuracy in determining fluid exit ratio. Each section, except the fourth arch sections, were split into two or three sections in order to obtain a more accurate area measurement.

a. Top third of the ceratobranchial

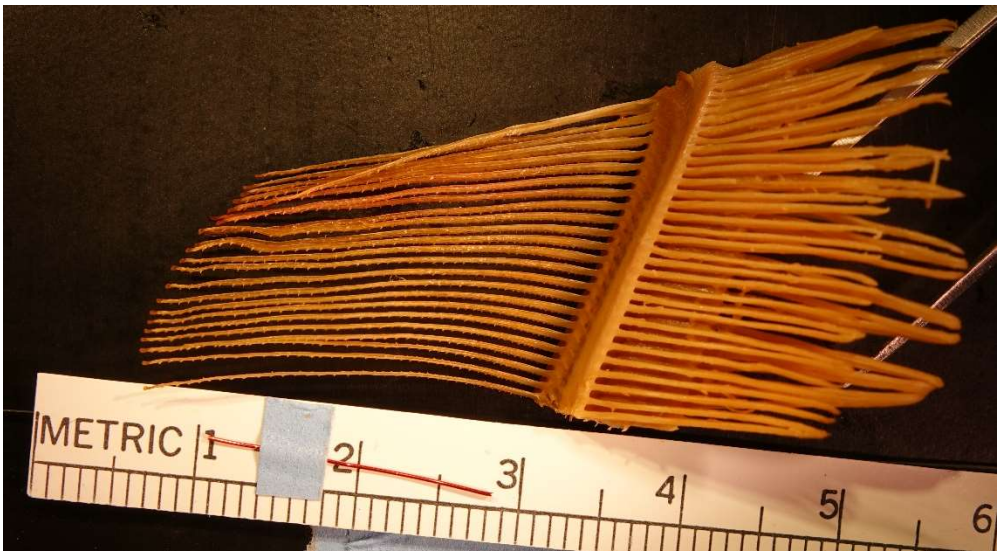

b. Middle third of the ceratobranchial

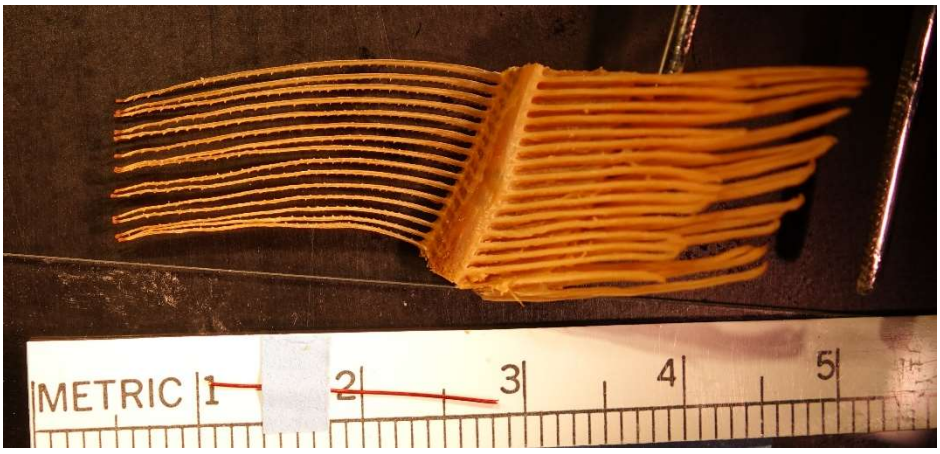

c. Lower third of the ceratobranchial

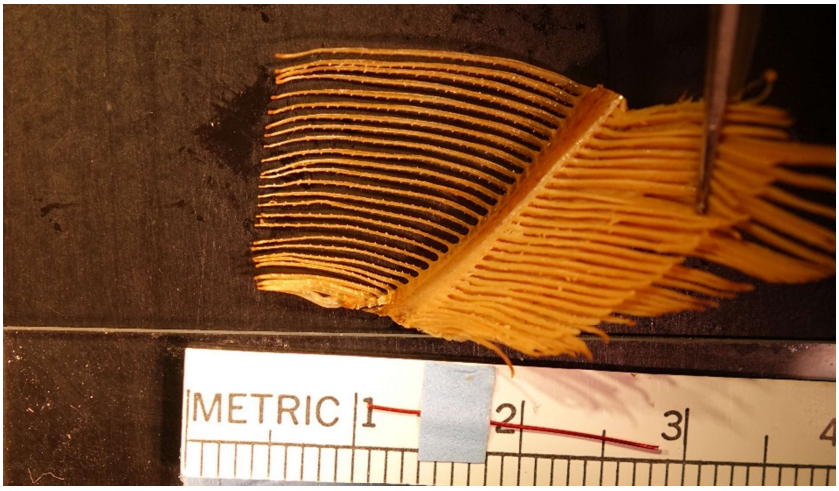

Figure 6. Lacunarity curves using the circular and square windows for each arch and section. The natural logarithm of the moving window size (the radius or the side length) is plotted on the x-axis, and the natural logarithm of the lacunarity is plotted on the y-axis.

a.

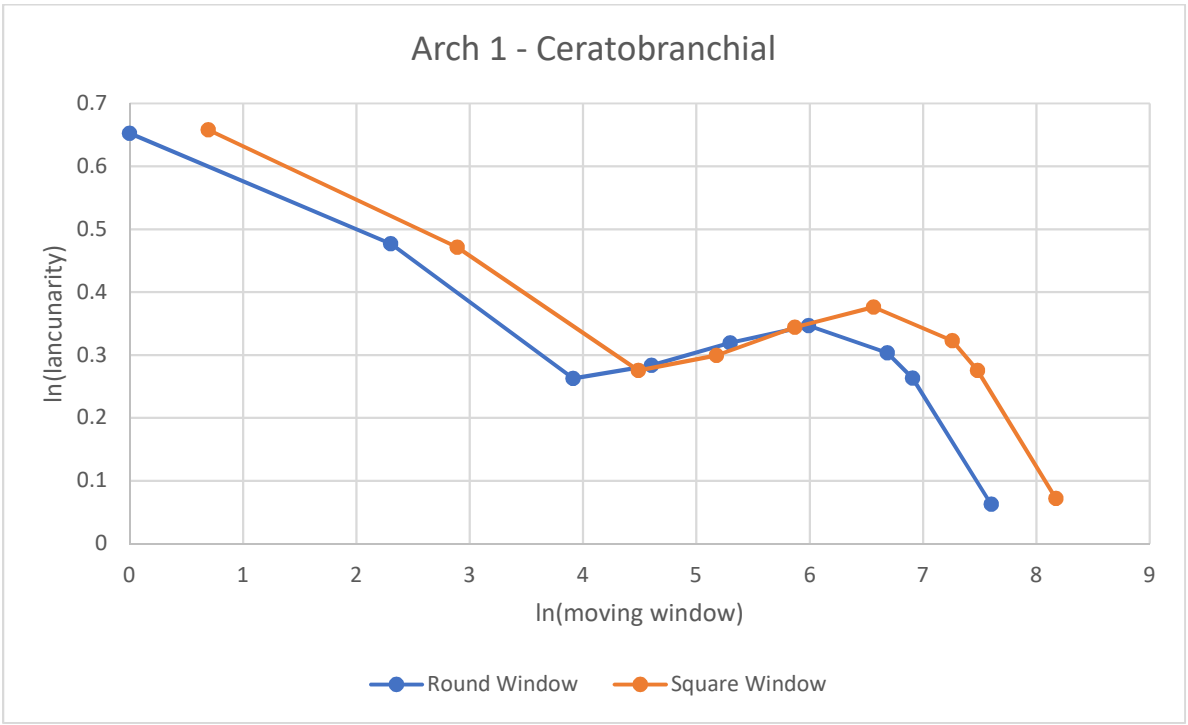

b.

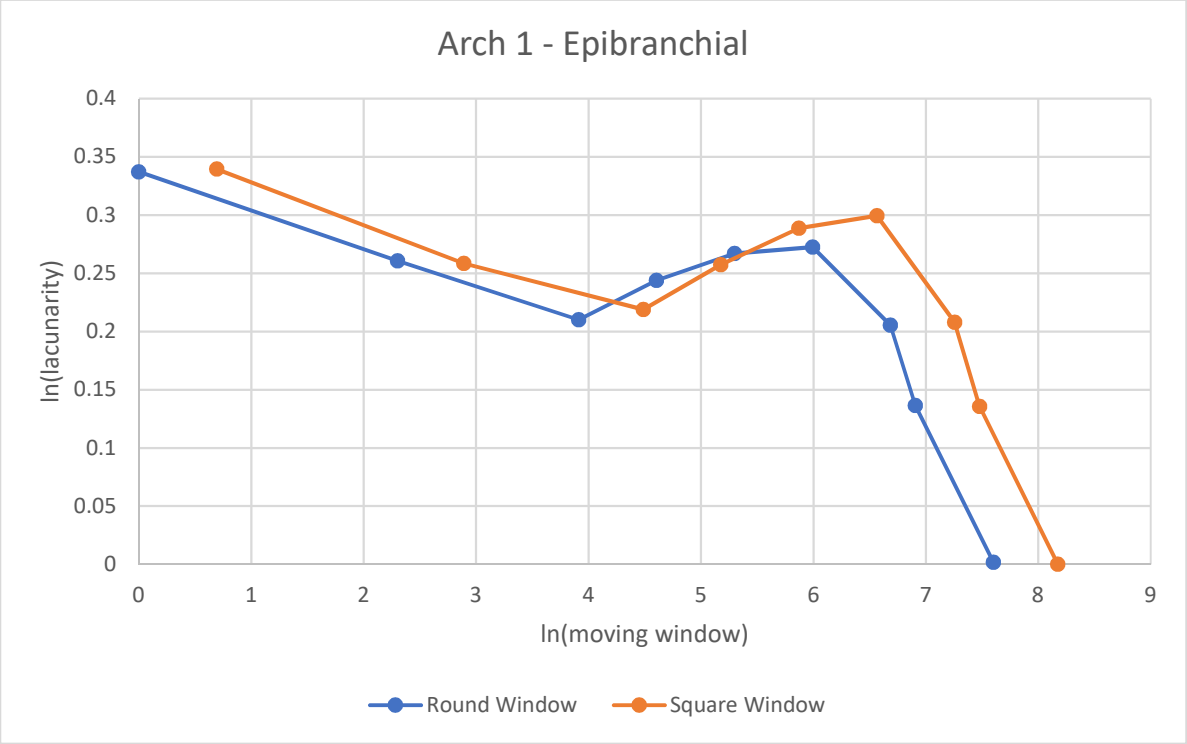
Arch 1 - Epibranchial
ln(lacunarity)
0.4
0.35
0.3
0.25
0.2
0.15
0.1
0.05
0
0 1 2 3 4 5 6 7 8 9
ln(moving window)
Round Window
Square Window

c.

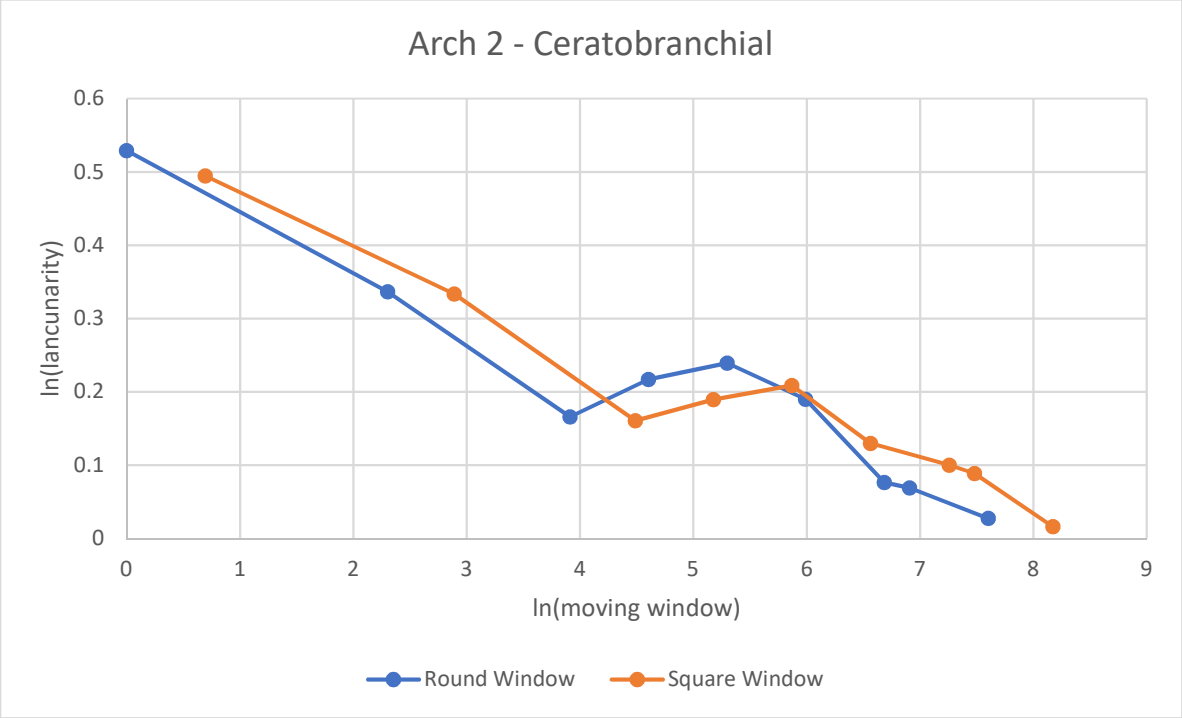
Arch 2 - Ceratobranchial
ln(lancunarity)
0.6
0.5
0.4
0.3
0.2
0.1
0
0 1 2 3 4 5 6 7 8 9
ln(moving window)
Round Window
Square Window

d.

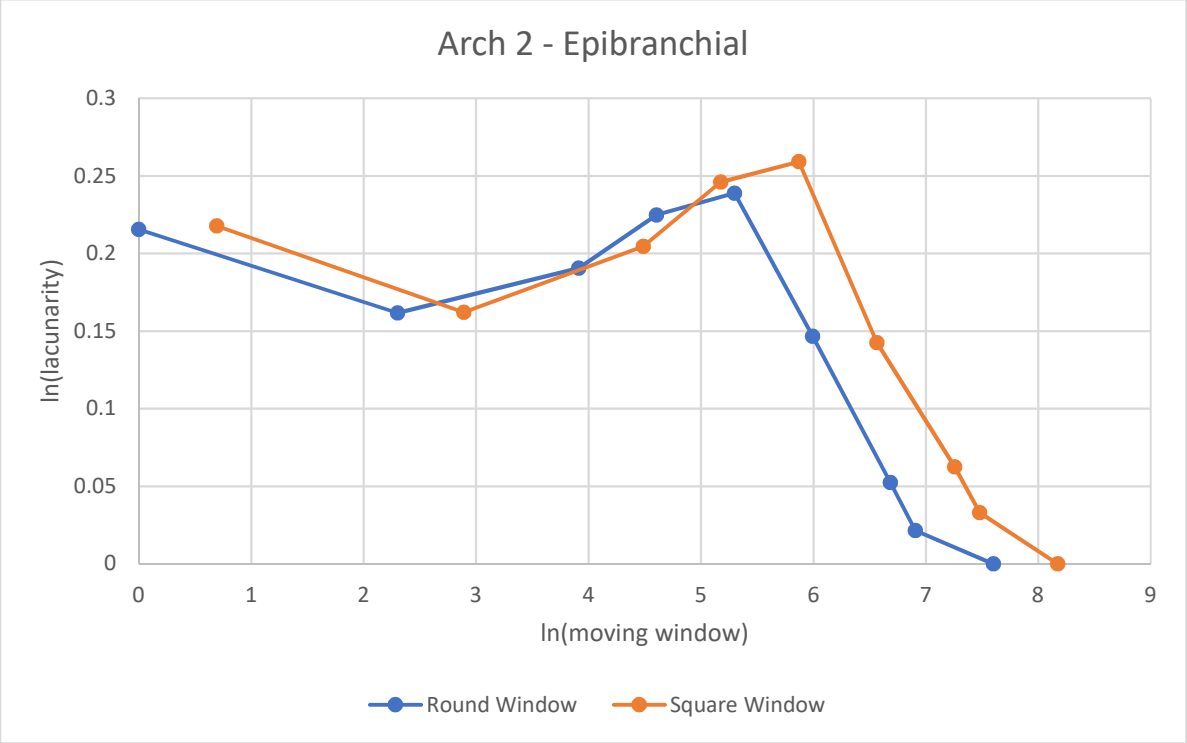
Arch 2 - Epibranchial
0.3
0.25
0.2
0.15
0.1
0.05
0
ln(lacunarity)
0
1
2
3
4
5
6
7
8
9
ln(moving window)
Round Window
Square Window

e.

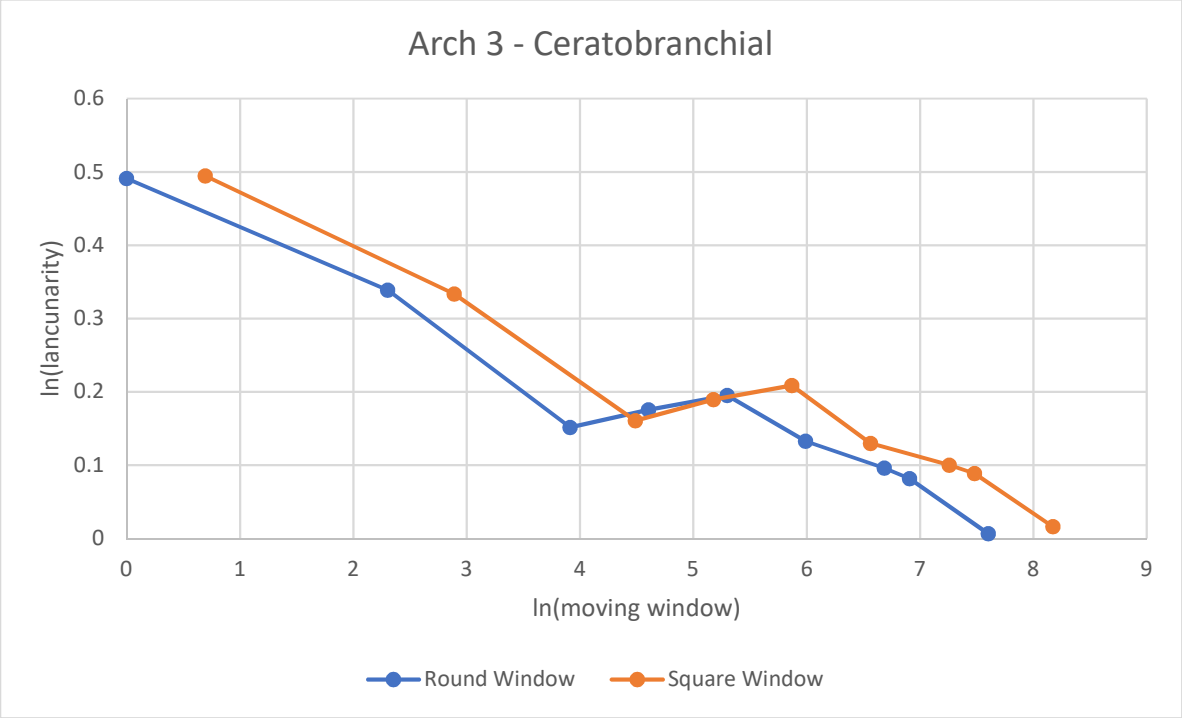
Arch 3 - Ceratobranchial
0.6
0.5
0.4
0.3
0.2
0.1
0
ln(lancunarity)
0
1
2
3
4
5
6
7
8
9
ln(moving window)
Round Window
Square Window

f.

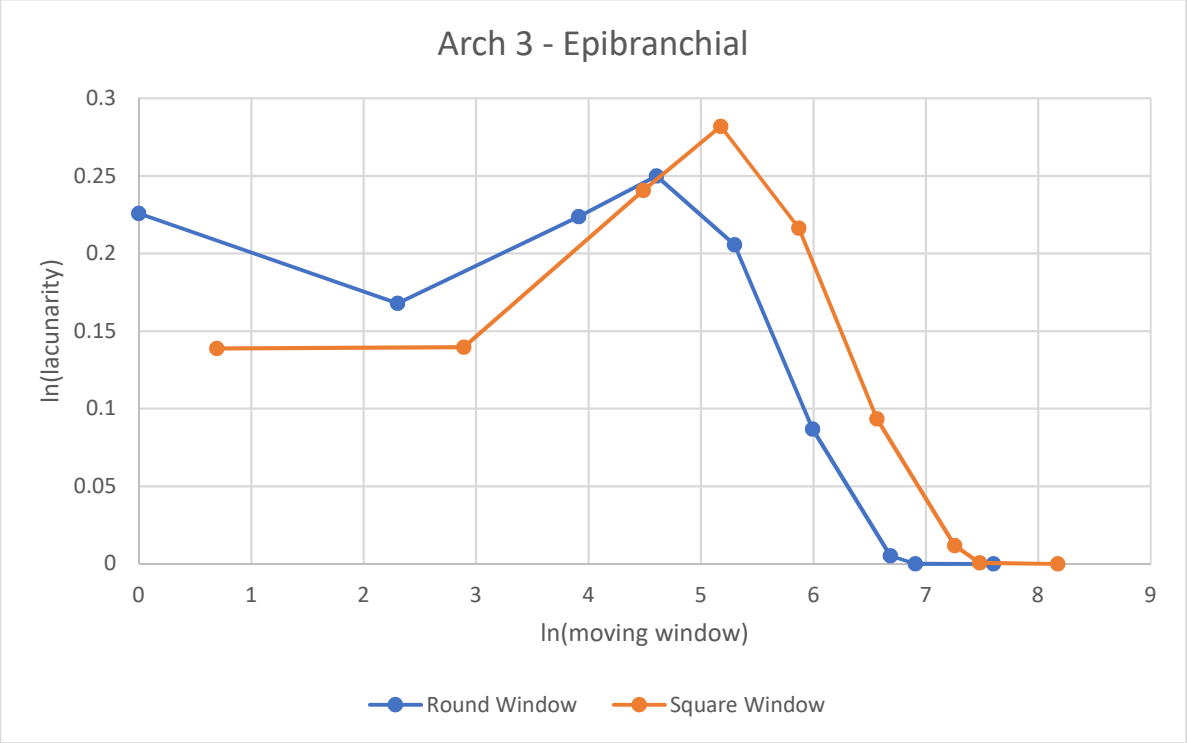
Arch 3 - Epibranchial
ln(lacunarity)
0.3
0.25
0.2
0.15
0.1
0.05
0
0
1
2
3
4
5
6
7
8
9
ln(moving window)
Round Window
Square Window

g.

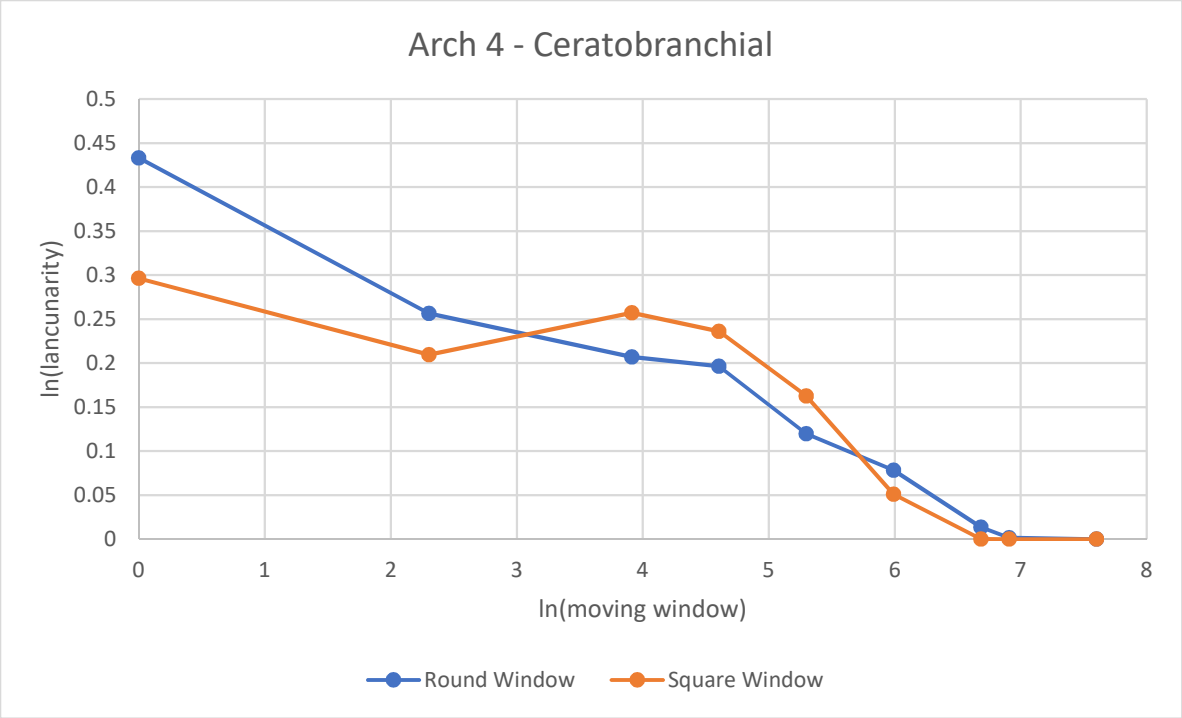
Arch 4 - Ceratobranchial
0.5
0.45
0.4
0.35
0.3
0.25
0.2
0.15
0.1
0.05
0
ln(lancunarity)
0
1
2
3
4
5
6
7
8
ln(moving window)
Round Window
Square Window

h.

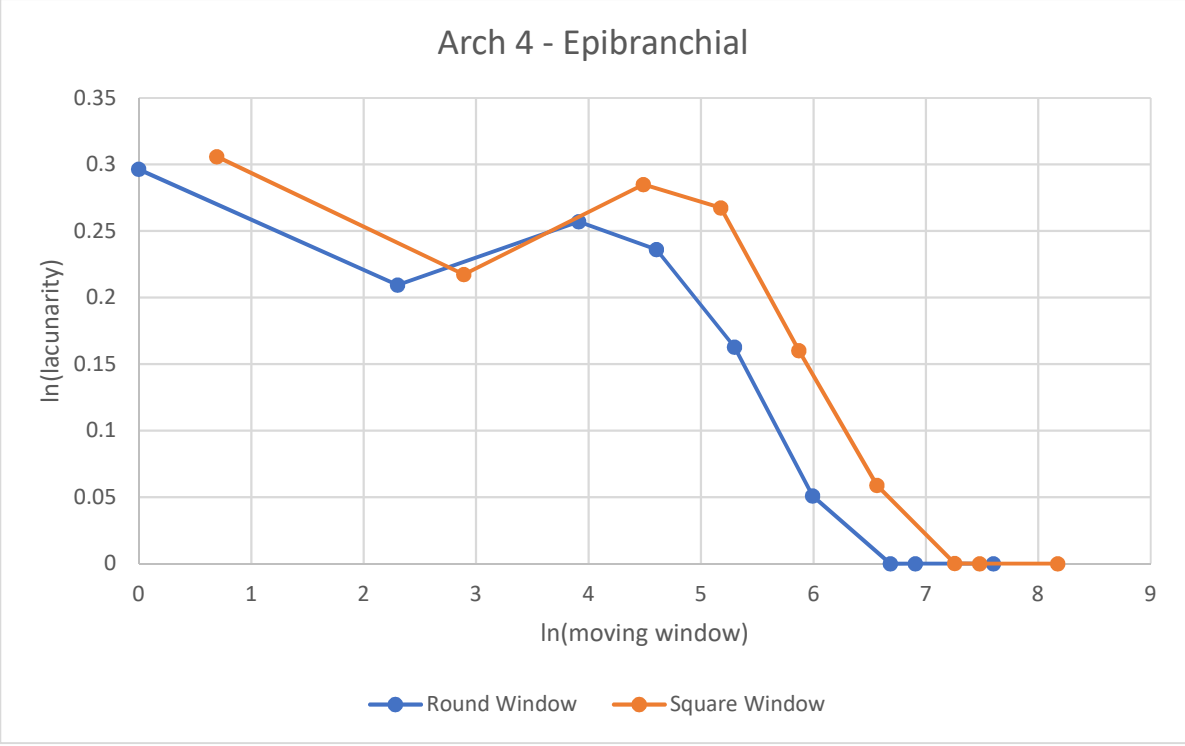
Arch 4 - Epibranchial
0.35
0.3
0.25
0.2
0.15
0.1
0.05
0
ln(lacunarity)
0
1
2
3
4
5
6
7
8
9
ln(moving window)
Round Window
Square Window

Figure 7. Normalized lacunarity curves for the ceratobranchial and epibranchial sections in each arch. Each curve was normalized by dividing all values in the series by the maximum value in the series. The natural logarithm of the moving window size (the radius or the side length) is plotted on the x-axis, and the natural logarithm of the normalized lacunarity is plotted on the y-axis.

a.

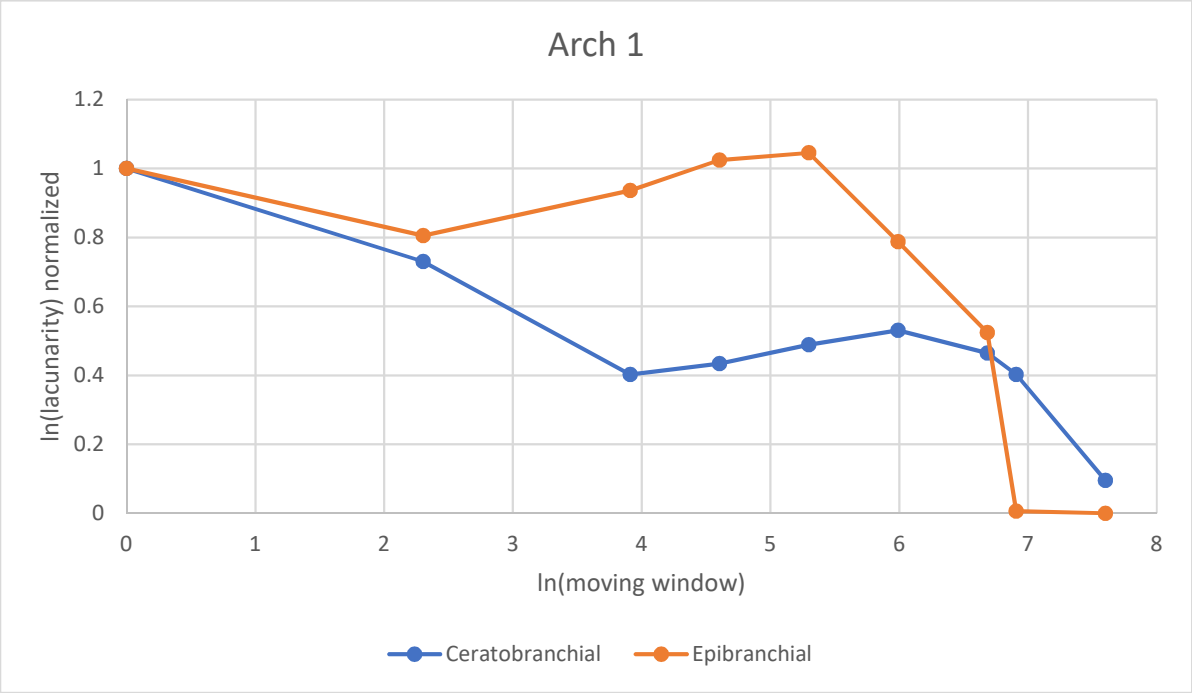

b.

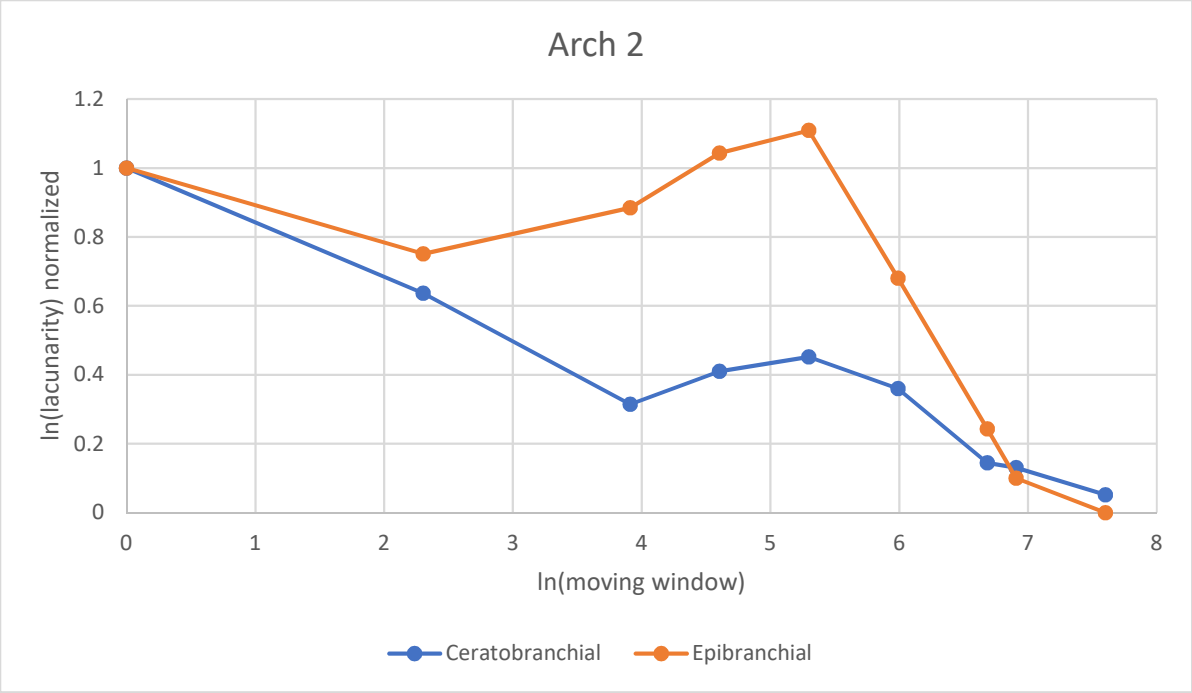
Arch 2
ln(lacunarity) normalized
1.2
1
0.8
0.6
0.4
0.2
0
0
1
2
3
4
5
6
7
8
ln(moving window)
Ceratobranchial
Epibranchial

c.

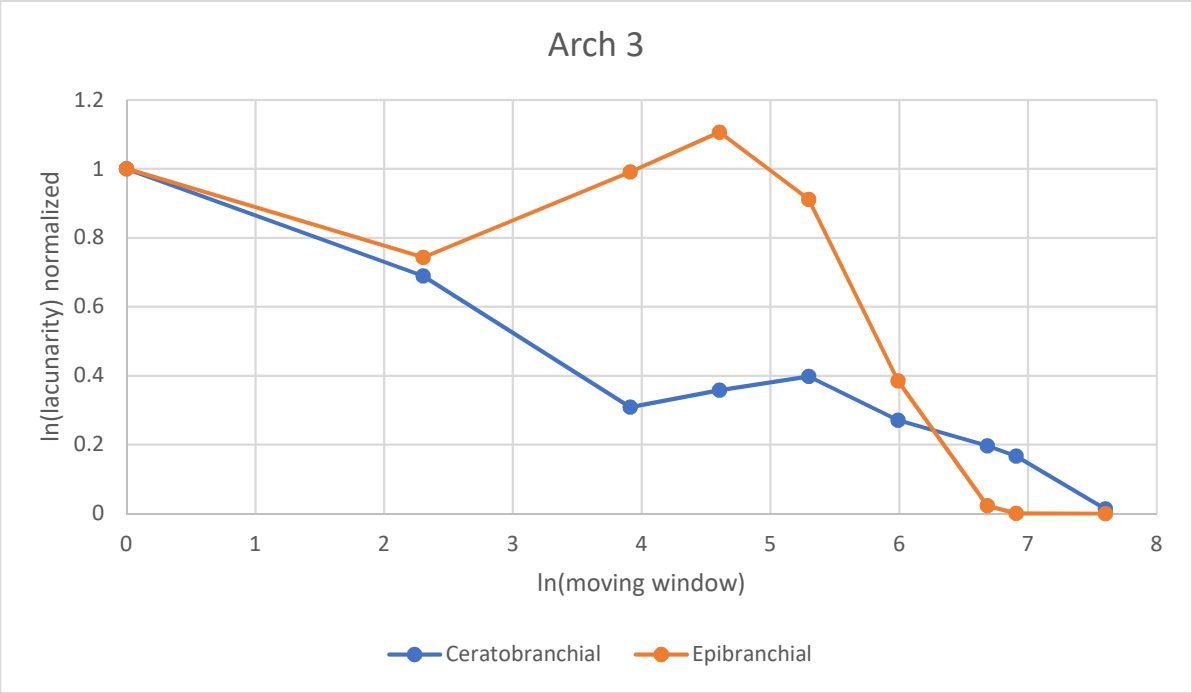
Arch 3
ln(lacunarity) normalized
1.2
1
0.8
0.6
0.4
0.2
0
0
1
2
3
4
5
6
7
8
ln(moving window)
Ceratobranchial
Epibranchial

d.

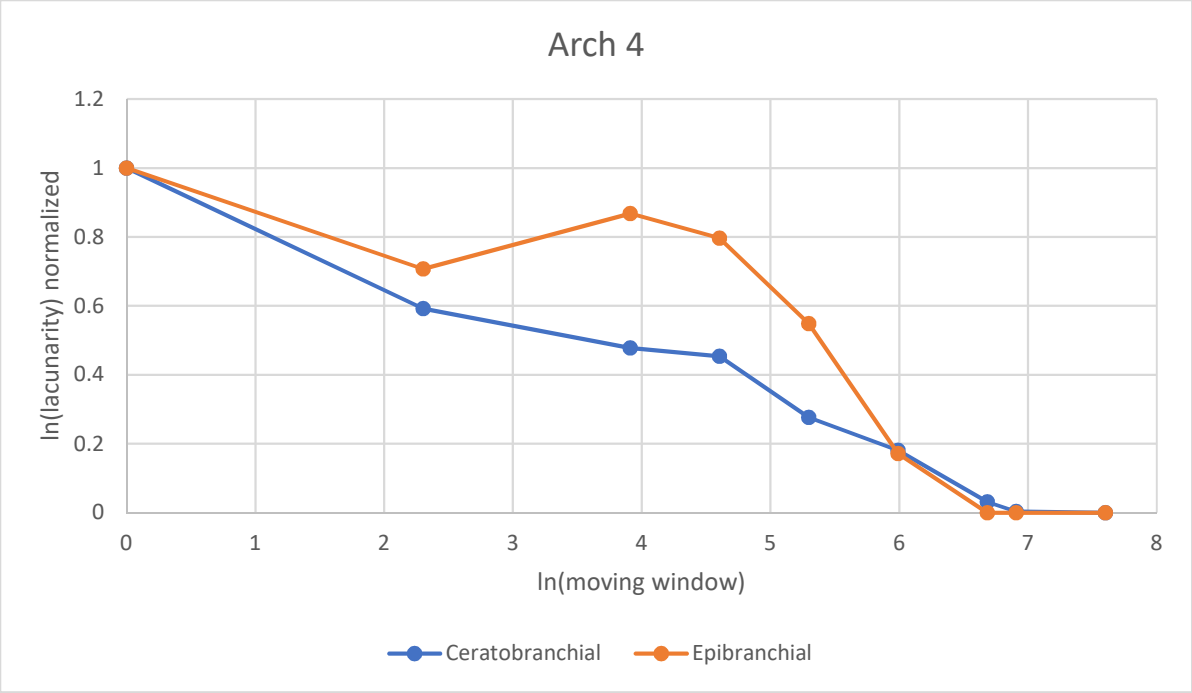

Figure 8. Lacunarity curves for the ceratobranchial section of each of the arches. The natural logarithm of the moving window size (the radius or the side length) is plotted on the x-axis, and the natural logarithm of the lacunarity is plotted on the y-axis.

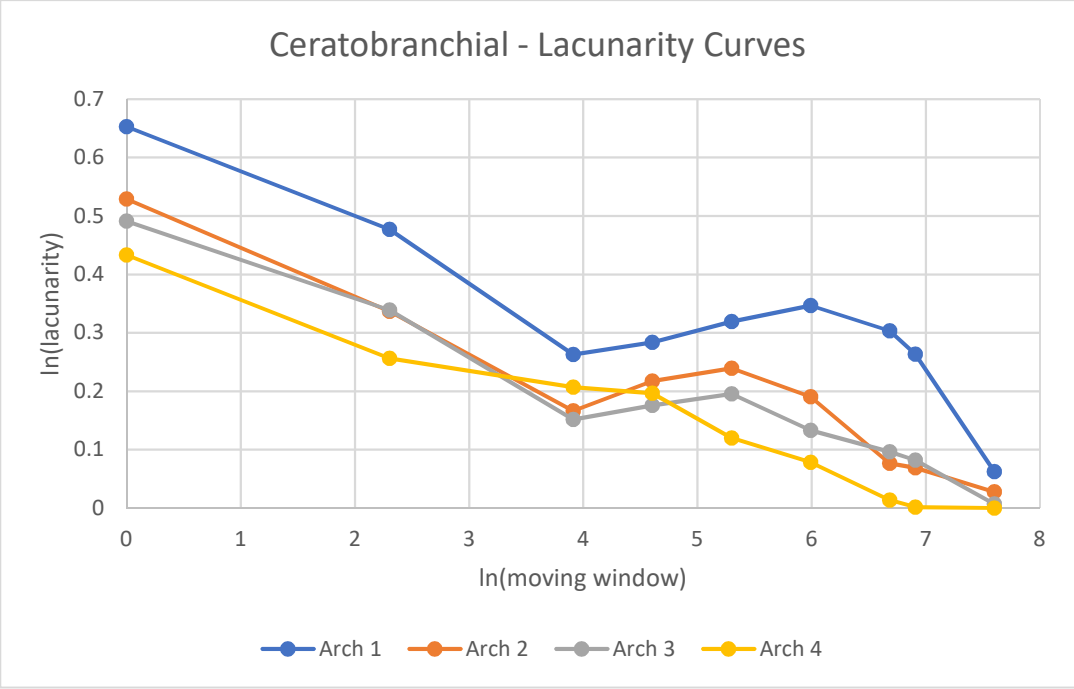

Figure 9. Lacunarity curves for the epibranchial section of each of the arches. The natural logarithm of the moving window size (the radius or the side length) is plotted on the x-axis, and the natural logarithm of the lacunarity is plotted on the y-axis.

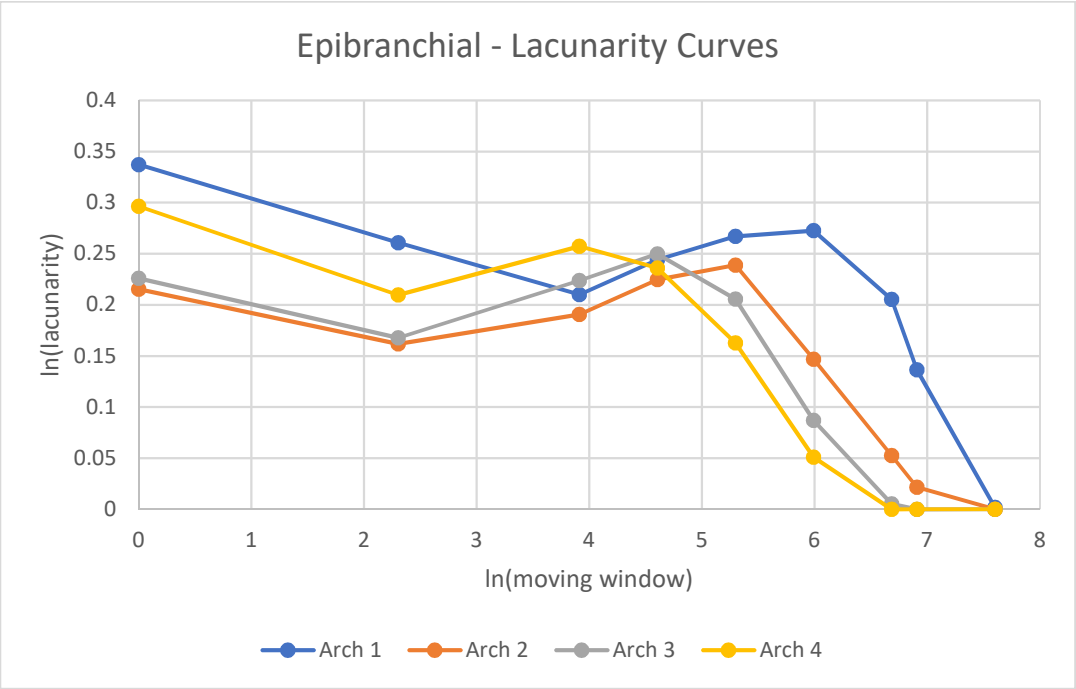

Figure 10. Close-up view of the rakers (arch 1 epibranchial portion) with the radius in cell size shown. The numbers are the length in cells of the black lines next to them. The 10 cell radius remains within the width of a raker while the rest of the radii extend across the width of a raker and into the space next to the raker.

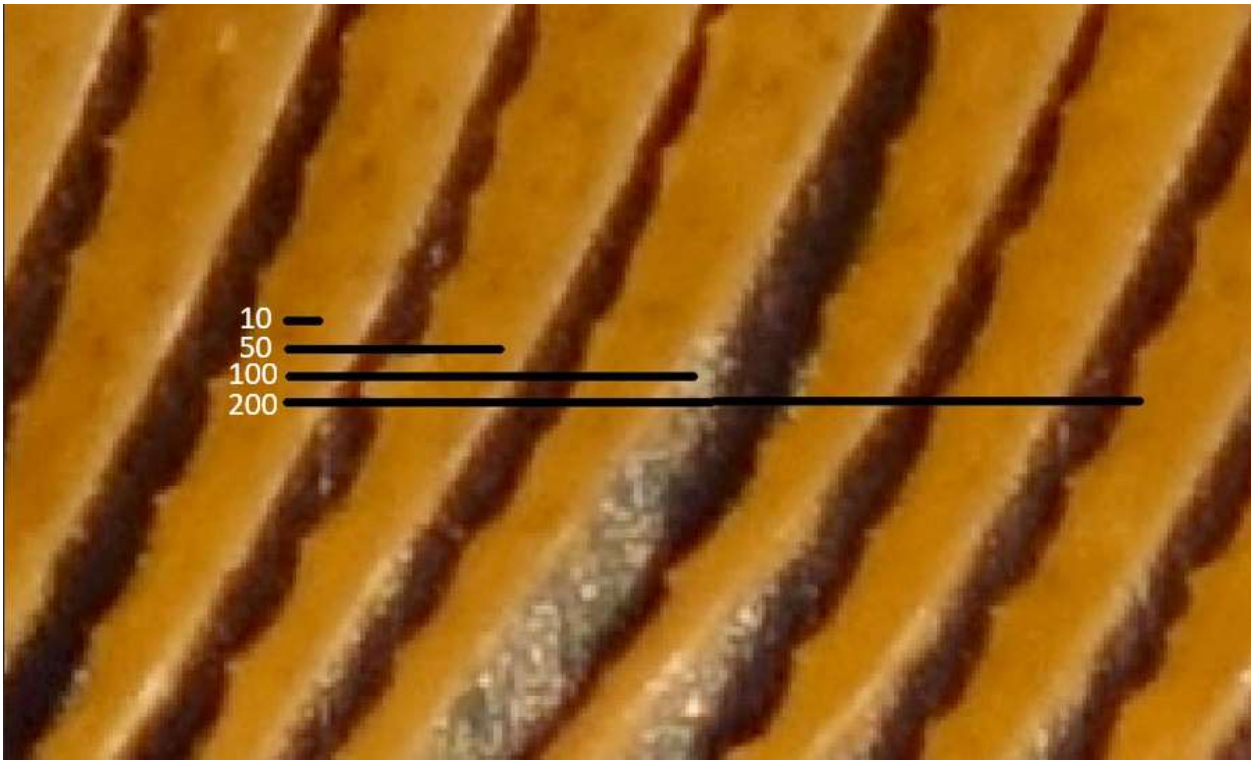

Tables

Table 1. Area measurements for the rakers, inter-raker space, total area, and percentages of each measurement. The area tends to decrease as the arch number increases but the percent raker area increases. The threshold values for the distinction between raker area and open space area are presented in Appendix A.

Arch	Raker Area (square mm)	Open Area (square mm)	Total Area (square mm)	Percent Raker Area	Percent Open Area
1	630.2448177	551.8107418	1182.055559	0.52688772	0.47311228
2	354.6971448	256.4299194	611.1270642	0.578538989	0.421461011
3	149.6601853	91.63210666	241.292292	0.621757645	0.378242355
4	79.18659781	43.38940662	122.5760044	0.644667232	0.355332768

Appendices

Appendix A. Threshold values for the distinction between the raker and open space area. Any values greater than or equal to the values in the table were classified as 1, or a raker, while remaining values were classified as 0, or empty space. The section name lists arch number; C for

ceratobranchial and E for epibranchial; low for lower region, mid for midsection, and top for upper section; 3 if the section was cut into thirds, 2 if the section was cut in half, and full if the section was not cut. For Arch 4 epibranchial section, the blue band was taken, and values less than or equal to 15 were counted as raker area.

Section	Threshold
1C low 3	125
1C mid 3	125
1C top 3	110
1E low 3	175
1E mid 3	100
1E top 3	150
2C low 3	100
2C mid 3	140
2C top 3	120
2E low 2	120
2E top 2	140
3C low 2	150
3C top 2	160
3E low 2	200
3E top 2	120
4C full	120
4E full	<=15